iScience

CellPress
OPEN ACCESS

Article

SERPINH1 modulates apoptosis by inhibiting P62 ubiquitination degradation to promote bone metastasis of prostate cancer

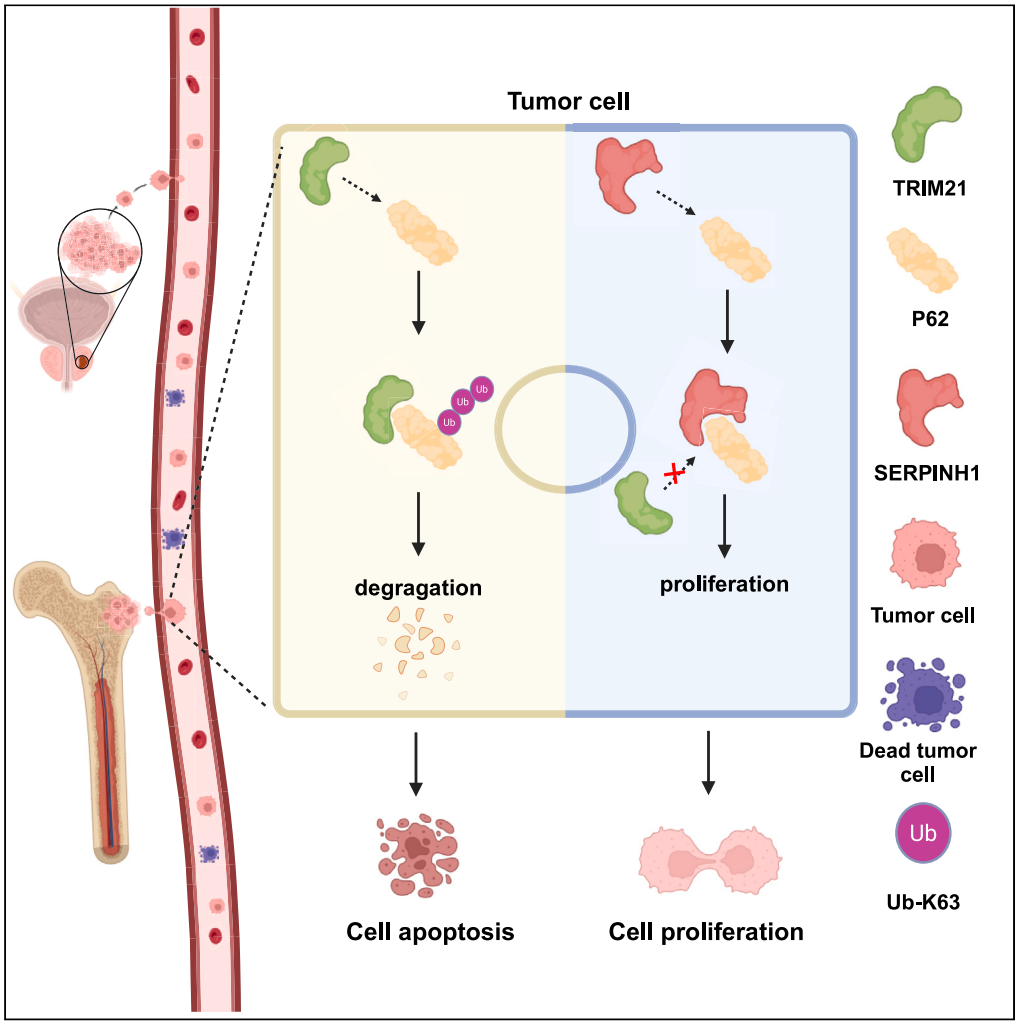

Chen Tang, Yiming Lai, Lingfeng Li, ..., Zhenghui Guo, Shengmeng Peng, Hai Huang

guozhhui@mail.sysu.edu.cn (Z.G.)
pengshm8@mail.sysu.edu.cn (S.P.)
huangh9@mail.sysu.edu.cn (H.H.)

Highlights

SERPINH1 inhibits P62 degradation via K63-linkage ubiquitination

SERPINH1 promotes PCa bone metastasis by suppressing P62-mediated apoptosis

Tang et al., iScience 27, 110427
August 16, 2024
https://doi.org/10.1016/j.isci.2024.110427

iScience

CellPress
OPEN ACCESS

Article

SERPINH1 modulates apoptosis by inhibiting P62 ubiquitination degradation to promote bone metastasis of prostate cancer

Chen Tang,[1,2,10] Yiming Lai,[1,3,4,5,10] Lingfeng Li,[1,3,10] Min-yi Situ,[6,10] Shurui Li,[7] Bisheng Cheng,[1,3] Yongming Chen,[8] Zhen Lei,[1,3] YanTing Ren,[9] Jie Zhou,[1,3] Yongxin Wu,[1,3] Haitao Zhong,[1,3] Kaiwen Li,[1,3,4] Lexiang Zeng,[1,3,4] Zhenghui Guo,[1,3,4,*] Shengmeng Peng,[1,3,4,*] and Hai Huang[1,3,4,5,11,*]

SUMMARY

Prostate cancer (PCa) is one of the most prevalent urogenital malignancies. Bone metastasis from PCa reduces patient survival rates significantly. There currently exists no effective treatment for bone metastatic PCa, and the underlying mechanisms remain unclear. This study performed transcriptomic screening on PCa bone metastasis specimens and intersection analysis in public databases and identified SERPINH1 as a potential target for treatment. SERPINH1 was found to be upregulated in PCa bone metastases and with poor prognosis, high Gleason score, and advanced metastatic status. SERPINH1 induced PCa cells' bone metastasis *in vivo*, promoted their proliferation, and mitigated apoptosis. Mechanistically, SERPINH1 bound to P62, reducing TRIM21-mediated K63-linked ubiquitination degradation of P62 and promoting proliferation and resistance to apoptosis of PCa. This study suggests the regulation of ubiquitination degradation of P62 by SERPINH1 that promotes PCa bone metastasis and can be considered as a potential target for treatment of bone metastatic PCa.

INTRODUCTION

Prostate cancer (PCa) is a prevalent form of urogenital malignancy. The prognosis of PCa patients varies widely. For localized PCa, the 5-year survival rate is 100%, but it is only 29.8% for metastatic PCa. The axial skeleton is where PCa cell metastasis occurs most frequently, accounting for approximately 90% of all reported cases. Bone metastasis is commonly associated with decreased physical function, loss of voluntary mobility, and reduced quality of life; pathological fractures and spinal cord compression are important skeletal-related events that can cause this condition. Due to its complex multistage process, the precise mechanism underlying bone metastasis in PCa is unknown. To infiltrate surrounding tissues, access microvasculature, breach blood sinus endothelium, enter the bone marrow stroma, and persist in the created "pre-metastasized niches," initial PCa cells must first undergo the epithelial-to-mesenchymal transition. The compositions of the extracellular matrix are altered by tumor cells by regulating the amount of collagen, fibrin, and other secreted substances, or secreting either transforming growth factor (TGF) or endothelin-1 to promote osteoblast differentiation and proliferation to remodel the bone microenvironment.[1,2] Insulin-like growth factor-1 (IGF-1) is secreted in response to increased osteoblast activity and supports the proliferation of PCa cells.[3] Activated osteoblasts release IGF-1 and increase PCa cell proliferation.[3] Nuclear factor kappa receptors-B ligand (RANK-L) can also encourage cancer cells to increase bone absorption, which releases bone matrix IGF-1 and TGF and promotes tumor cell proliferation as positive feedback.[4] Current treatments for bone metastasis mainly aim to prevent disease progression and release symptoms. In patients with PCa bone metastasis, targeted treatment such as RANK-L antagonist denosumab or osteoclast antagonist bisphosphonates enhances bone structure but not survival. Additionally, uncontrolled cell proliferation and prolonged cell survival significantly contribute to the formation of cancer, which can

[1]Department of Urology, Sun Yat-sen Memorial Hospital, Sun Yat-sen University, Guangzhou 510120, Guangdong, P.R. China
[2]Department of Urology, Huazhong University of Science and Technology Union Shenzhen Hospital, Shenzhen, Guangdong 518052, P.R. China
[3]Guangdong Provincial Key Laboratory of Malignant Tumor Epigenetics and Gene Regulation, Sun Yat-sen Memorial Hospital, Sun Yat-sen University, Guangzhou 510120, Guangdong, P.R. China
[4]Guangdong Provincial Clinical Research Center for Urological Diseases, Guangzhou 510120, Guangdong, P.R. China
[5]Department of Urology, the Fifth Affiliated Hospital of Xinjiang Medical University, Urumqi 830011, Xinjiang, P.R. China
[6]State Key Laboratory of Oncology in South China, Guangdong Provincial Clinical Research Center for Cancer, Sun Yat-sen University Cancer Center, Guangzhou 510060, P.R. China
[7]Sun Yat-sen Memorial Hospital, Sun Yat-sen University, Guangzhou 510120, Guangdong, P.R. China
[8]Beijing Hospital, National Center of Gerontology Institute of Geriatric Medicine, Chinese Academy of Medical Sciences, Peking Union Medical College, Beijing, Dongcheng, P.R. China
[9]Department of Pathology, Sun Yat-sen Memorial Hospital, Sun Yat-sen University, Guangzhou 510120, Guangdong, P.R. China
[10]These authors contributed equally
[11]Lead contact
*Correspondence: guozhhui@mail.sysu.edu.cn (Z.G.), pengshm8@mail.sysu.edu.cn (S.P.), huangh9@mail.sysu.edu.cn (H.H.)
https://doi.org/10.1016/j.isci.2024.110427

spread throughout the body via circulation.[5] The proliferative and anti-apoptotic abilities of cancer cells significantly contribute to tumor growth.

SERPINH1 was initially identified as an endoplasmic reticulum retention protein that prevents abnormal collagen secretion under stress during collagen processing and quality control.[6] Abnormal expression of SERPINH1 is associated with osteogenic defect, scarring, and fibrosis, among others.[7] Recent research has revealed a connection between aberrant SERPINH1 expression and the oncogenesis of malignancies. Indeed, Yang et al. suggested a link between the degree of neuroblastoma malignancy and SERPINH1 expression.[8] Breast cancer cells may also interact with platelets and cause lung metastasis and colonization via enhancing SERPINH1 expression.[9]

In humans, sequestosome 1 (SQSTM1) (or P62) has been implicated in inflammation, oncogenesis, autophagy, apoptosis, and oxidative stress.[10–15] P62 expression is significantly elevated in prostate,[14] liver,[15] and lung cancer cells.[16] Yu et al. reported that human cisplatin-resistant ovarian cancer cells SKOV3/Cisplatin (DDP) expressed P62 at a significantly greater level than cisplatin-sensitive SKOV3 cells[17]; P62 also prevents endoplasmic-reticulum-stress-induced apoptosis, thereby inducing tumor cells resistant to cisplatin chemotherapy. Takamura et al. revealed that autophagy suppression-induced liver tumors were considerably reduced by the simultaneous inactivation of P62 and Nrf2.[18] In human hepatocellular carcinoma, P62 is the primary component of improperly accumulating inclusions; the TRAF2-p62 axis promotes proliferation and survival of liver cancer by activating mTORC1 pathway.[19,20] By inactivating the P62/Keap1/Nrf2 pathway, NEDD4L inhibits the progression and promotes the apoptosis of Bladder cancer (BLCA).[21] P62/NBR1 Liquid droplet inhibited the lung metastasis of A549 cells in murine model.[22] However, uncertainty remains regarding the regulation mechanisms of P62 in PCa. One of the most significant post-translational alterations of biological and pathological processes is ubiquitination. The tripartite motif containing-21 (TRIM21) ubiquitin E3 ligase is substantially abundant in hepatocellular carcinoma; furthermore, TRIM21 deletion enhances the isolation of Keap1 and P62 and protects cancer cells from the impacts of diethylnitrosamine (DEN)-induced reactive oxygen species and mortality.[23] Jin et al. suggested that interferon-β enhances the ubiquitination of P62 via the ISGylation of TRIM21 and blocks its autophagosome targeting.[24]

Here, this research found that SERPINH1 has a high expression level in PCa bone metastases, which is correlated with an aggressive tumor state and a worse prognosis. We also established that SERPINH1 positively regulates P62 through their interaction and subsequently inhibits TRIM21-mediated ubiquitination degradation of P62. Finally, we demonstrated that SERPINH1 increases PCa bone metastasis by promoting PCa cell proliferation and preventing apoptosis. Our findings are beneficial for a deeper understanding of the function of SERPINH1 in PCa, which has significant potential clinical implications.

RESULTS

Intersection analysis of bone metastasis-related genes in PCa datasets and RNA sequencing

Bone metastases in PCa patients are fatal. We explored our Sun Yat-Sun University (SYSU)-RNA sequencing dataset, a proteomics dataset established by our research group, a GEO dataset (GSE77930), and a proteomics dataset (Diego proteomics from *Clinical Cancer Research*) to screen biomarkers for PCa bone metastasis. SYSU-RNA sequencing intersection analysis identified 167 differentially expressed genes. SYSU proteomics also identified 3,059 bone metastases-expressed proteins over the detection threshold. The GSE77930 datasets comparing primary PCa and bone metastases yielded 2,535 differentially expressed genes. Diego proteomics identified 2,408 differentially expressed proteins in bone metastases. Intersection analysis of the four datasets revealed five differentially elevated genes (Figure S1A). SERPINH1 was one of the intersection genes and exhibited a high expression level in PCa bone metastases and indicated a worse prognosis (Figures S1B–S1E).

Elevated expression of SERPINH1 is found in metastatic PCa tissue and is correlated with a poor prognosis

Immunohistochemistry was used to identify SERPINH1 expression in PCa tissues from 103 SYSUCC patients to determine its clinical relevance. Table S1 outlines the patients' clinical features. SERPINH1 exhibited exceedingly high expression level in metastatic PCa compared to localized PCa (Figure 1A), and it has higher expression in PCa with a high Gleason score (Gleason score = 9) than normal and lower-Gleason-score paracancer tissue (Figures 1B and 1C). High SERPINH1 expression was correlated with greater T staging, lymph node metastasis, distant metastasis, and Gleason score (Figures 1D–1F). Further Kaplan-Meier analysis revealed that elevated SERPINH1 expression is related to inferior progression-free and overall survival (Figures 1G and 1H). In addition, univariate and multivariate analysis of clinicopathologic indicators identified SERPINH1 as an independent risk factor (Tables S2 and S3). In conclusion, SERPINH1 is related to a worse prognosis and a more severe tumor grade in PCa, according to our data.

SERPINH1 enhances PCa cells proliferation *in vitro* and bone metastasis *in vivo*

We designed two efficient small interfering RNAs (siRNAs) targeting the coding sequence region of SERPINH1 to assess the physiology of SERPINH1 in PCa cells and constructed stable cell lines of PC3 and DU145 that overexpressed SERPINH1 using lentivirus. Quantitative reverse-transcription PCR (RT-qPCR) and western blotting examined PCa cell SERPINH1 knockdown or overexpression. PC3 and DU145 cell lines with SERPINH1 knockdown or overexpression had significantly lower or higher mRNA and protein levels than the control group, respectively (Figures 2A and 2B). CCK8 and colony-formation tests showed that SERPINH1 knockdown decreased PC3 and DU145 cell proliferation and colony formation, whereas overexpression had the opposite effect (Figures 2C and 2D). But transwell assay showed no significance after knockdown of SERPINH1 (Figure S1F).

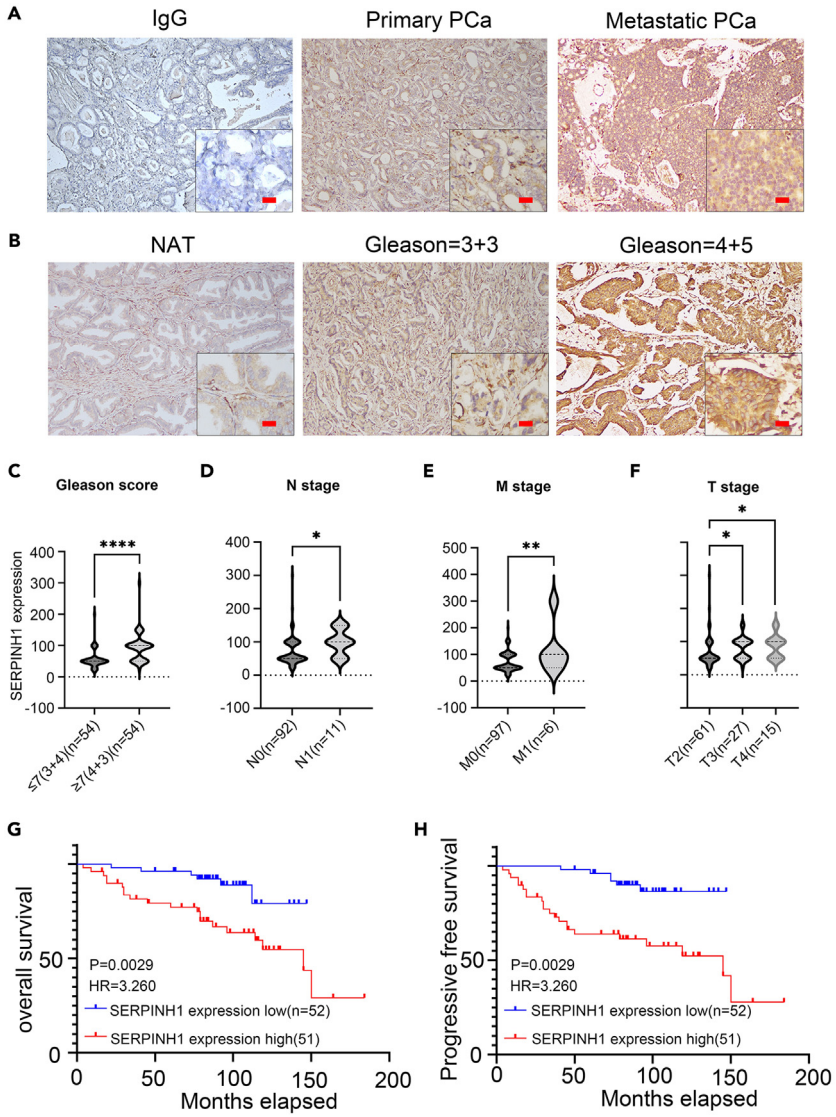

Figure 1. SERPINH1 exhibits a high expression level in metastatic PCa tissue and is associated with a worse prognosis

(A) Typical images of immunohistochemistry staining of SERPINH1 at the primary and metastatic PCa. Red scale bars measure 50 μm.

(B) Typical images of SERPINH1 between NAT and PCa tissue with low and high Gleason scores. Red scale bars measure 50 μm.

(C) Differential expression of SERPINH1 between different Gleason scores in PCa.

(D) Differential expression of SERPINH1 between lymph node-negative (N0) and node-positive (N1) PCa.

(E) Differential expression of SERPINH1 between primary (M0) and distantly metastatic (M1) PCa.

(F) Differential expression of SERPINH1 with different T stages.

(G) OS Kaplan-Meier curves for SERPINH1 levels in PCa.

(H) Progression-free survival (PFS) Kaplan-Meier curves for SERPINH1 levels in PCa. Data are represented as mean ± SD. (*$p < 0.05$, **$p < 0.01$, ****$p < 0.0001$).

To explore the influence of SERPINH1 on PCa cell metastatic capacity *in vivo*, we constructed two short hairpin RNA (shRNA)-mediated stable knockdown PC3-luciferase cell lines, SERPINH1#sh1 and SERPINH1#sh2, and a stable overexpression of SERPINH1 PC3-luciferase cell line, SERPINH1-overexpression (OE), using lentivirus. We performed an intra-caudal artery injection bone metastasis xenograft in nude mice based on prior studies.[25] Bioluminescent imaging (BLI) revealed that SERPINH1 knockdown decreased the BLI signals (Figures 3A and 3B) and bone metastases formation rate (Figure 3C). SERPINH1 knockdown reduced bone lesions on X-ray and μCT (Figures 3A and S2A). Four positive bone metastasis nude mice were formed in the control group, with a bone metastases formation rate of 66.7%, and two were formed in each SERPINH1 knockdown group, with a bone metastases formation rate of 33.3%. Meanwhile, SERPINH1 overexpression significantly increased the BLI signals (Figures 3D and 3E) and bone metastases formation rate (Figure 3F). Four positive bone metastasis nude mice were formed in the control group, with a bone metastases formation rate of 66.7%, and six were formed in the SERPINH1 overexpression

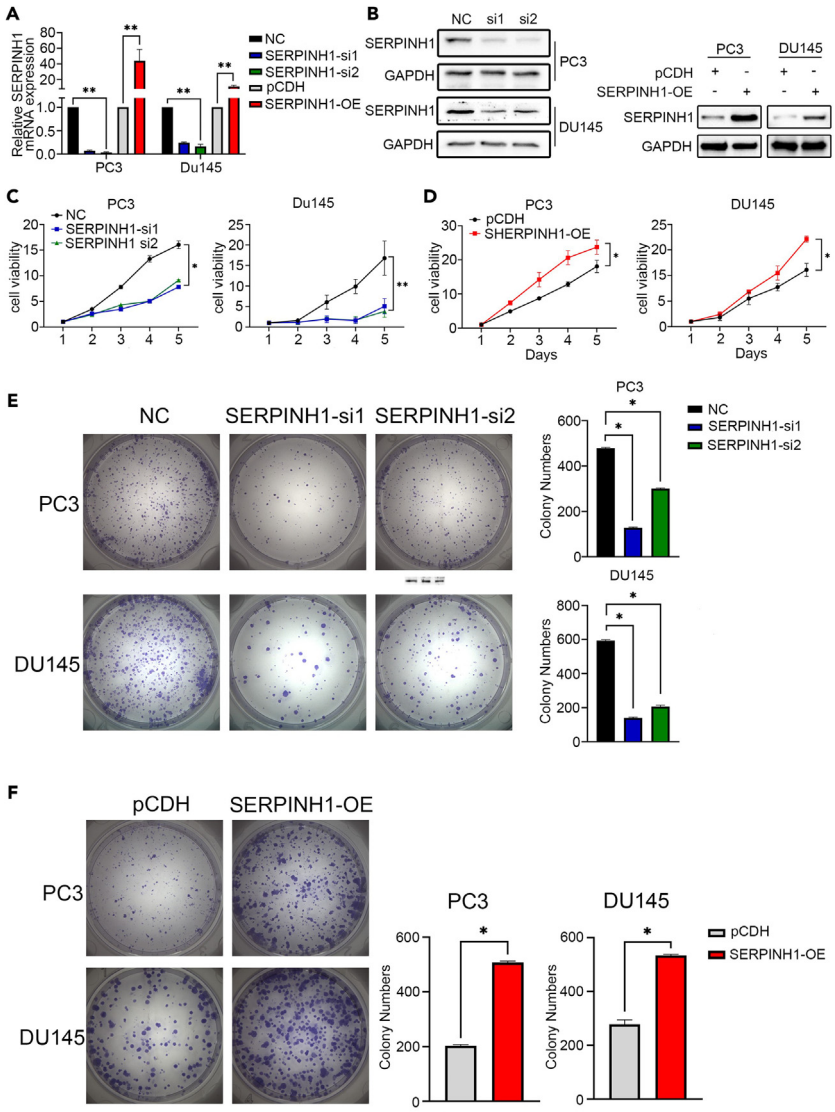

Figure 2. SERPINH1 promotes PCa cell proliferation *in vitro*

(A) mRNA levels of SERPINH1 in knockdown or overexpressed cells.

(B) Protein expression levels of SERPINH1 in PCa cells.

(C and D) Cell viability of SERPINH1 knockdown or overexpressing cells.

(E and F) Colony formation assays of SERPINH1 knockdown or overexpressing cells. Histograms of colony-formation assay. Data are represented as mean ± SD. (*$p < 0.05$, **$p < 0.01$).

group, with a bone metastases formation rate of 100%. X-ray analysis revealed that SERPINH1 overexpression increased bone lesions (Figure 3D). The knockdown group expressed the least SERPINH1 and the OE group the most (Figure S2B). The SERPINH1 knockdown group had considerably less bone damage than the normal group, while the overexpression group had the opposite result (Figure S2B). Immunofluorescence staining showed that, after knockdown of SERPINH1, ratio of Ki-67+ proliferative PCa cells decreased than that of the scramble group in tumor tissues (Figure S3A).

SERPINH1 knockdown induces PCa cells apoptosis *in vitro*

We observed evident cell death in SERPINH1 knockdown cells. To determine how SERPINH1 induces cell death, we applied an Annexin V/propidium iodide (PI) double-stain apoptotic assay and found more double-staining cells in SERPINH1 knockdown cells (Figure 4A). Then, to explore the mechanism by which SERPINH1 induces cell death, we treated SERPINH1 knockdown cells with Quinoline-Val-Asp-Difluorophenoxymethylketone (Q-VD-OPH) (an apoptosis inhibitor). Q-VD-OPH drastically decreased double-staining apoptotic cells in SERPINH1 knockdown cells (Figure 4B). SERPINH1 also protected PC3 and DU145 cells against apoptosis when exposed to the apoptosis

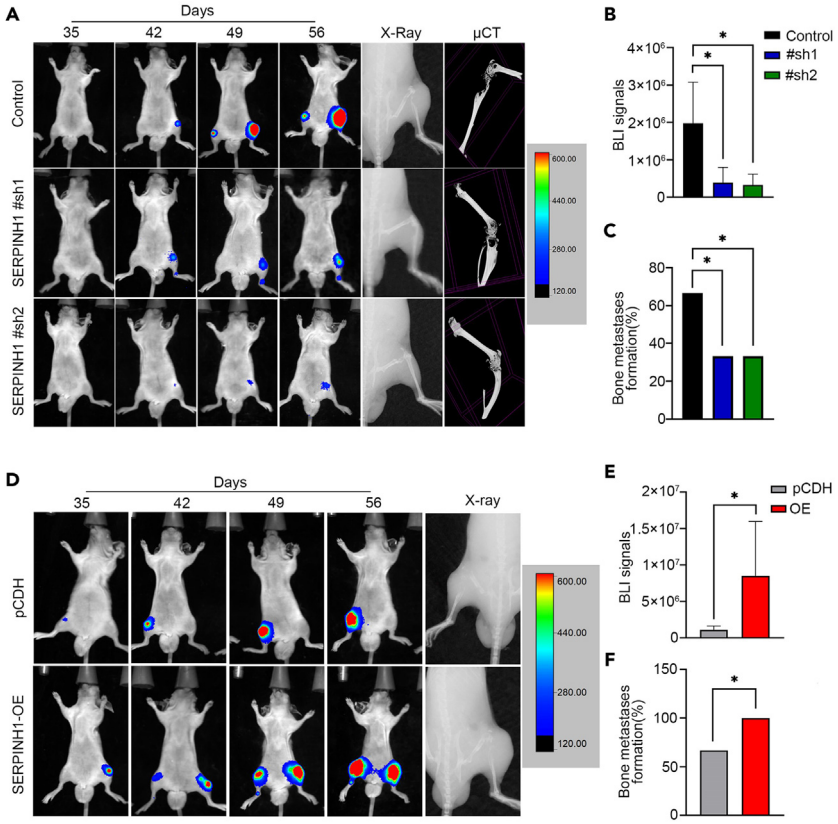

Figure 3. SERPINH1 promotes PCa cell bone metastasis *in vivo*

(A) Bioluminescence, X-ray, and μCT images of caudal artery injection bone metastases in the PC3-luc-SERPINH1#sh1, PC3-luc-SERPINH1#sh2, and PC3-Luc-scramble groups.

(B) Bone metastases BLI signals in the SERPINH1 knockdown group.

(C) Bone metastases formation rate in each group ($n = 6$).

(D) Bioluminescence and X-ray images of caudal artery injection bone metastases in the PC3-Luc-pCDH and PC3-Luc-SERPINH1-OE groups.

(E) Bone metastases BLI signals in the SERPINH1 overexpression group.

(F) Bone metastases formation rate in both groups ($n = 6$). Data are represented as mean ± SD. (*$p < 0.05$, **$p < 0.01$, ***$p < 0.001$, ****$p < 0.0001$).

inducer SM-164 + tumor necrosis factor alpha (TNF-α) for 48 h (Figure 4C). We also determined the apoptosis *in vivo*. In TUNEL assay, apoptotic PCa cells ratio increased after knockdown of SERPINH1 in tumor tissues (Figure S3B).

SERPINH1 is located in the endoplasmic reticulum and plays a role as collagen-specific molecular chaperones in collagen biosynthesis. Next, we explored whether SERPINH1-dependent collagen secretion contributes to the apoptosis. Type I collagen (COL1) was the most abundant collagen in tumor stroma and reported as a regulator in the metastatic event mediated by SERPINH1.[26] Flow cytometry showed that the exogenous addition of COL1 could not inhibit the apoptosis reduced by knockdown of SERPINH1, which imply that SERPINH1-dependent collagen secretion does not contribute to the process (Figure S4C).

SERPINH1 interacts with P62 in PCa cells

The co-immunoprecipitation (coIP) and mass spectrometry (MS) were applied to research the SERPINH1 overexpressed PC3 and DU145 cell lines and identified 114 and 49 SERPINH1-specific binding proteins, respectively. P62 was identified via a crossover of the MS results of the two cell lines (Figures 5A, S4A, and S4B). Western blotting and coIP revealed SERPINH1-P62 interaction in PC3 and DU145 cells (Figure S5A). To validate the interaction of SERPINH1 and P62, we co-transfected Glutathione-S-transferase (GST) or GST-SERPINH1 into 293T cells and performed GST pull-down assay. Western blotting showed that P62 was detected in GST-SERPINH1 but not the GST complex (Figure 5B). Immunofluorescence showed intracellular co-localization of SERPINH1 and P62 in PCa cells (Figure 5C). Fluorescence resonance energy transfer (FRET) assay also proved the interaction between SERPINH1 and P62 (Figure 5D). These data suggest that SERPINH1 interacts with P62 in PCa cells.

SERPINH1 affects the stability of P62 by inhibiting its ubiquitination

Given the close interaction between SERPINH1 and P62, we investigated whether SERPINH1 affects the P62 protein level. Western blotting showed lower P62 protein expression after SERPINH1 knockdown and higher expression of P62 protein after SERPINH1 overexpression

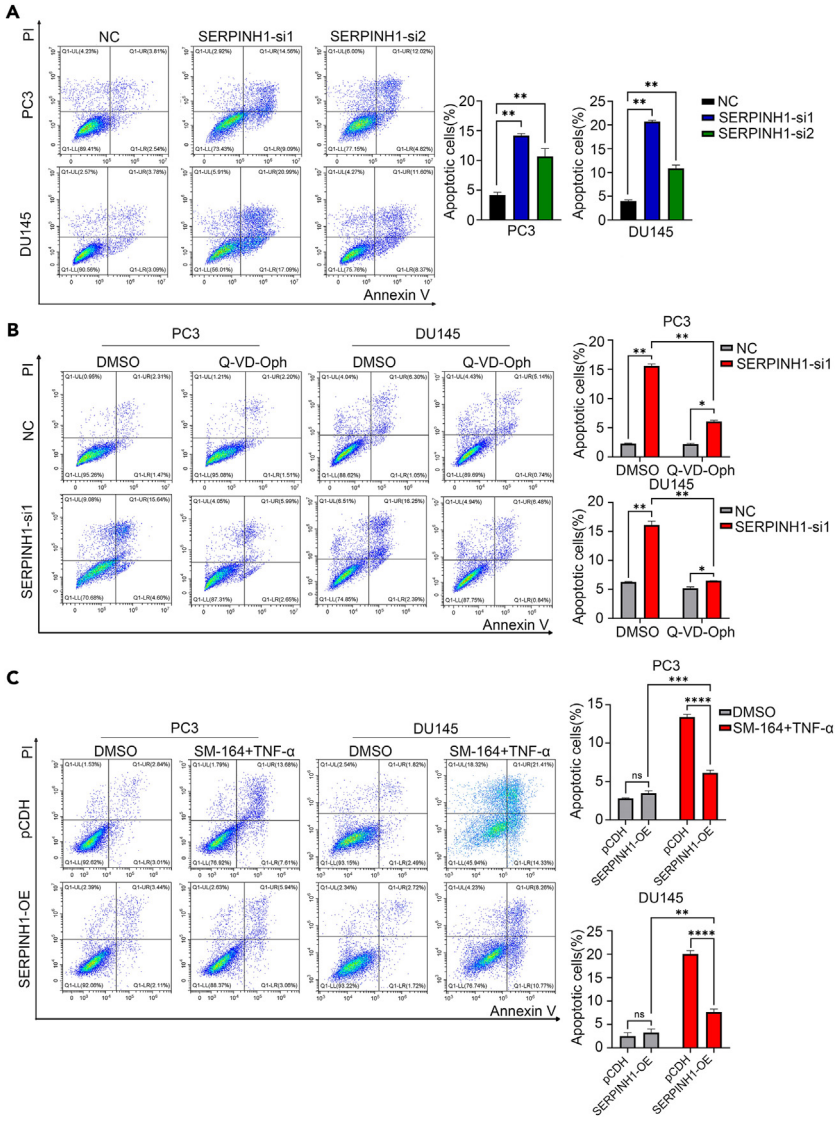

Figure 4. SERPINH1 regulates the apoptosis of PCa cells

(A) Cell death in SERPINH1 knockdown cells was detected by Annexin V/PI double-staining. Histograms of double-stained cells ratio.

(B) Annexin V/PI apoptotic assay of SERPINH1 knockdown cells and subsequent addition of the apoptotic inhibitor Quinoline-Val-Asp-Difluorophenoxymethylketone. Histograms of the ratio of double-stained cells.

(C) Annexin V/PI apoptotic assay of PCa cells treated with SM-164 + TNF-α. Histograms of double-stained cells ratio. Data are represented as mean ± SD. (*$p < 0.05$, **$p < 0.01$, ***$p < 0.001$, ****$p < 0.0001$).

(Figures 5E and S5B). However, the quantity of P62 protein in SERPINH1 knockdown cells was discordant with its mRNA (Figure 5F), suggesting that SERPINH1 has a post-translational regulatory effect on P62.

The protein synthesis inhibitor cycloheximide (CHX) was used to measure the rate of P62 degradation in SERPINH1 knockdown cells to ascertain if SERPINH1 influences the stability of P62. SERPINH1 knockdown decreased P62 expression and greatly shortened its half-life while overexpression of SERPINH1 increased P62 half-life under the CHX treatment (Figures 5G and S5C). These findings suggest that SERPINH1 impacts P62 protein stability. When MG132, a proteasome inhibitor, was applied to SERPINH1 knockdown cells, it prevented the P62 protein level decline, suggesting that SERPINH1 may regulate P62 proteasome degradation (Figure 5H). Consistently, overexpression of SERPINH1 synergistically inhibits the P62 proteasome degradation with MG132 (Figure S5C). To determine whether SERPINH1 regulates P62 degradation via ubiquitination, we transfected the hemagglutinin (HA)-tagged ubiquitin plasmid into PCa cells and conducted coIP of P62 and western blotting. SERPINH1 knockdown cells had enhanced P62 polyubiquitination (Figure 5I). Overexpression of SERPINH1 attenuated P62 polyubiquitination (Figure S5E). Collectively, SERPINH1 regulates P62 protein levels by protecting P62 from ubiquitination-proteasome-mediated protein degradation.

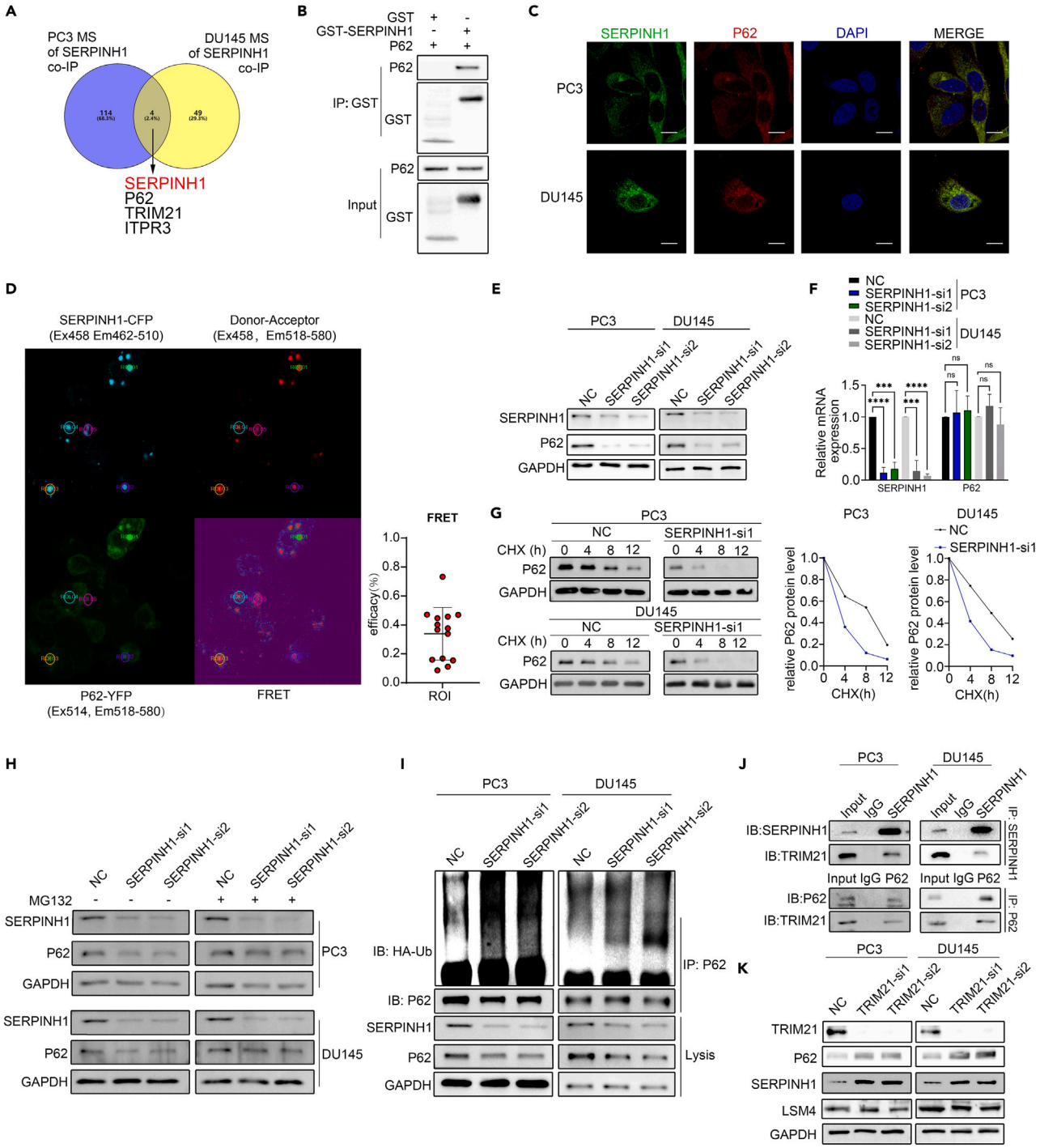

Figure 5. SERPINH1 interacts with P62 and protects P62 from TRIM21-mediated ubiquitination

(A) Intersection analysis of PC3 and DU145 cells mass spectrometry of SERPINH1 coIP.

(B) GST pull-down assay to determine the interaction of SERPINH1 with P62 in PC3 and DU145 cell lines.

(C) Immunofluorescence of SEPPINH1 and P62 in PCa cells. The white scale bar measures 10 μm.

(D) FRET analysis showed the proteins interaction of SERPINH1 and P62.

(E) P62 protein level in SERPINH1 knockdown cells.

(F) P62 mRNA level in SERPINH1 knockdown cells.

(G) P62 protein level in SERPINH1 knockdown cells at indicated times following cycloheximide (CHX) treatment (20 μg/mL).

(H) P62 protein level in SERPINH1 knockdown cells following treatment of MG132 for 12 h (10 μg/mL).

Figure 5. *Continued*

(I) The HA-tagged polyubiquitination level of P62 in SERPINH1 knockdown cells.

(J) CoIP results of SERPINH1 and TRIM21.

(K) Protein levels of SERPINH1 and P62 in TRIM21 knockdown cells, LSM4 set as an irrelative protein to exclude the influence of knockdown TRIM21 to other protein. Data are represented as mean ± SD. (*$p < 0.05$, **$p < 0.01$, ***$p < 0.001$, ****$p < 0.0001$).

SERPINH1 protects P62 against TRIM21-mediated K63-linkage ubiquitination and subsequently promotes PCa cells' bone metastasis

The most significant and highly selective protein degradation mechanism in eukaryotes is ubiquitination-proteasome-mediated protein degradation. Typically, ubiquitin ligase E3 exerts a key role in ubiquitination. The crossover of MS of SERPINH1 in two PCa cell lines identified an E3 ligase, TRIM21 (Figure S6A), which interacts with various intracellular molecules. CoIP demonstrated that both SERPINH1 and P62 could interact with TRIM21 (Figure 5J).

To verify whether SERPINH1 or P62 is a ubiquitination substrate of TRIM21, we first detected the protein level of SERPINH1 and P62 in TRIM21 knockdown PCa cells and found that TRIM21 knockdown increased the levels of SERPINH1 and P62 proteins (Figure 5K). Moreover, SERPNH1 knockdown increased exogenous HA-tagged K63-linkage ubiquitylation of P62 in PCa cells (Figure 6A) instead of K48-linked or K11-linked ubiquitination of P62 (Figures S7A and S7B). Considering the interaction between P62 and SERPINH1, we hypothesized that SERPINH1 may form a protein dimer with P62 and subsequently impair the interaction between P62 and TRIM21 and protect P62 against TRIM21-mediated ubiquitination degradation. We transfected increasing concentrations of SERPINH1-Flag into PC3 cells to confirm this hypothesis. SERPINH1 elevation substantially reduced P62-TRIM21 interaction (Figure 6B), while a knockdown of SERPINH1 significantly increased the interaction (Figure 6C). Moreover, we detected the expression of SERPINH1 and P62 in bone metastases in mice via immunohistochemical staining, finding that P62 was significantly decreased in SERPINH1 knockdown and increased in SERPINH1-overexpressed bone metastases (Figure 6D). Our results suggest that SERPINH1 regulates the stability of P62 by preventing its TRIM21-mediated K63-linkage ubiquitination and degradation, thereby causing the accumulation of P62 in PCa cells and promoting PCa bone metastasis.

The effects of SERPINH1 knockdown on proliferation and apoptosis are recovered by P62 overexpression

P62 is a signaling hub involved in various cell functions; hence interference with the regulation of P62 can affect cell survival, cell death, and oxidative stress. To determine whether SERPINH1 regulate PCa cell proliferation and apoptosis through P62, we designed two siRNAs targeting the coding sequence region of P62 and validated their biological significance. Colony-formation and cell counting kit (CCK8) assay results reflect that P62 silencing has an adverse influence on proliferation (Figures 7A–7C). Additionally, silencing P62 had a comparable effect to silencing SERPINH1 in inducing apoptosis in PCa cells (Figures 7D and 7E). P62 overexpression reversed cell growth and apoptosis after SERPINH1 knockdown (Figures 7F–7H), while SERPINH1 or P62 knockdown enhanced the apoptotic protein cleaved-caspase-8 (Figures S7C–S7E), indicating that the anti-apoptotic mechanism of SERPINH1 in PCa may include the P62-caspase8 axis.

DISCUSSION

Evidence for both "seed-soil" idea and "vicious cycle" hypothesis as explanations for how bone metastases develop has been reported. According to the "seed-soil" idea, various growth factors, neovasculature, cytokines, and chemokines in bone tissue function as "soil" to assist tumor cells proliferate during bone metastasis.[27] The "vicious cycle" theory claims that when tumor cells are introduced to bone tissue, the dynamic equilibrium between osteoclasts and osteoblasts is interrupted, and TGF and endothelin-1 from tumor cells stimulate osteoblast proliferation and differentiation and affect the bone microenvironment. The bloodstream is where circulating tumor cells (CTCs) spread to other distant organs after metastasis. The presence of CTCs in PCa indicates the existence of early-stage bone metastasis before the onset of clinical bone metastases.[28] Studies have shown a correlation between PCa diagnosis and prognosis with the amount and type of CTCs in a patient's blood circulation.[29] When PCa cells enter the blood circulation and become CTC, they undergo programmed cell death, including apoptosis, necrosis, pyroptosis, and ferroptosis, induced by various factors. Furthermore, tumor cells produce endothelin-1 and TGFs to modify the bone microenvironment and promote osteoblast differentiation and proliferation.[30,31] The capacity of tumor cells to withstand apoptosis and boost proliferation is necessary for their survival in the circulatory system and their reactivation following hibernation in the skeletal microenvironment. There are perspectives which suggest that apoptosis inhibits metastatic dissemination through the elimination of misplaced cells. The viability of the metastatic process is dependent on the capacity of malignant cells to evade apoptosis. Resistance to apoptosis is critical in every stage of metastatic advancement.[32] A few studies have showed that apoptosis promotes the metastasis of cancer. A study in 2018 points out that, apoptosis PCa cells induced the expression of proinflammatory cytokines such as CXCL5 by activating Stat3 and nuclear factor κB (NF-κB) (p65) signaling and accelerates the inflammation and tumor growth in bone.[33] In colorectal cancer, ANGPTL4 inhibits apoptosis and promotes metastasis of colorectal cancer cells by upregulation of bone morphogenetic protein 7 (BMP7).[34] Inhibition of NF-κB signaling and integrin-β1 attenuates osteosarcoma metastasis via increased cell apoptosis[35]; inactivation of Stat3 signaling by bortezomib induces apoptosis and suppresses cell growth and metastasis in chondrosarcoma.[36] These studies indicated a correlation and underlaying mechanism of apoptosis with metastasis. In this study, we found that SERPINH1, a serine protease inhibitor superfamily member, was upregulated during PCa bone metastasis. The aberrant expression of SERPINH1 is associated with osteogenesis imperfecta, scarring, and fibrosis.[7] The endoplasmic reticulum, cytoplasm, and cell membrane are major locations of SERPINH1; it enters the extracellular space via secretion. Abnormal SERPINH1 expression is closely related to oncogenesis, and the degree of neuroblastoma is

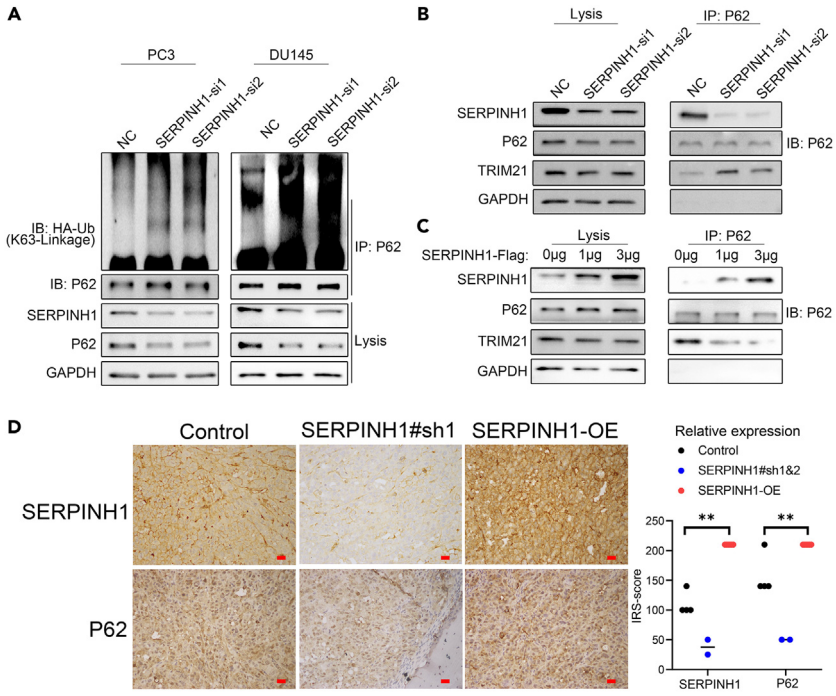

Figure 6. SERPINH1 promotes PCa metastasis by competitively binding to P62 and inhibiting its TRIM21-mediated K63-linkage ubiquitination

(A) K63-linkage HA-tagged polyubiquitination of P62 in SERPINH1-knockdown group.

(B) CoIP assay of P62 in SERPINH1 overexpressing group.

(C) CoIP assay of P62 in SERPINH1-overexpressed PCa cells.

(D) Representative immunohistochemistry staining and quantification diagram of SERPINH1 and P62 of each group. Data are represented as mean ± SD. (*$p < 0.05$, **$p < 0.01$, ***$p < 0.001$, ****$p < 0.0001$).

strongly linked with the level of SERPINH1 expression.[8] By upregulating SERPINH1, breast cancer cells improve tumor cell-platelet interaction and promote lung metastasis and colonization.[9] In addition, SERPINH1 promotes metastasis by binding to non-muscle myosin IIA and inositol-requiring transmembrane kinase endoribonuclease-1α, thereby increasing the secretion of collagen and fibronectin.[37] Hepatic stellate cells became more sensitive to endoplasmic reticulum stress and apoptosis after SERPINH1 knockdown.[38]

This study found that SERPINH1 promote bone metastasis *in vivo* and proliferation *in vitro* of PCa cells. Knockdown of SERPINH1 expression led to apoptosis of PCa cells, while overexpression of SERPINH1 resisted apoptosis induced by SM-164 + TNF-α. Additionally, SERPINH1 interacted with P62 and protected it against proteasomal degradation. Based on our cohort ($n = 103$) and open datasets, SERPINH1 was overexpressed in bone metastases. Strong SERPINH1 expression in PCa was associated with a worse prognosis, more metastatic spread, and a higher Gleason grade. For patients with PCa, SERPINH1 may predict poor disease-free survival and represent a bone metastasis PCa treatment target.

Apoptosis helps evolve and maintain the intracellular environment. However, tumor cells undergo an aberrant apoptotic process involving numerous signaling pathways and various chemicals. P62 participates in the maintenance and regulation of various fundamental cellular activities, including apoptosis, and prevents endoplasmic-reticulum-stress-induced apoptosis, thereby causing cancer cell resistance to cisplatin chemotherapy. P62 expression is significantly elevated in the PCa cells [14], Megan A. et al. showed that high-P62 bone metastasis PCa cell lines were resistant to bone marrow stromal cell-induced apoptosis and autophagy.[39] In this study, P62 was involved in SERPINH1 knockdown-induced PCa cell apoptosis. Several researches have studied how P62 impacts apoptosis. Zhao et al. reported that caspase 8 was activated by Oroxylin A and subsequently proteolyzes P62 (SQSTM1) to produce apoptosis,[40] while Yu et al. discovered that P62 exerts a key function in the activation of caspase 8 based on increasing ovarian cancer cells susceptibility to cisplatin.[17] Similarly, our study demonstrated that SERPINH1 knockdown induces activation of caspase 8, thus triggering apoptosis of PCa cells.

Multiple processes can enhance protein expression, including transcriptional upregulation and prevention of protein breakdown. This paper found that the P62 protein level was regulated by SERPINH1; nevertheless, the underlying method by which this occurs remains to be clarified. Given the close interaction between SERPINH1 and P62, SERPINH1 may regulate P62 through post-translational modification. P62 is a ubiquitin-binding scaffold protein implicated in autophagy and the ubiquitin-proteasome system.[41] It functions as an anchor to promote the degradation of unwanted molecules, and its ubiquitination modulates its autophagy activity; however, the degradation of P62 requires further research. Ferbian et al. revealed that Parkin ubiquitinated P62, causing its proteasomal degradation and subsequent low levels under hypoxic conditions.[42] Overexpression of ASB6 aided in the ubiquitination and destruction of P62, whereas CUL5 or ASB6 depletion

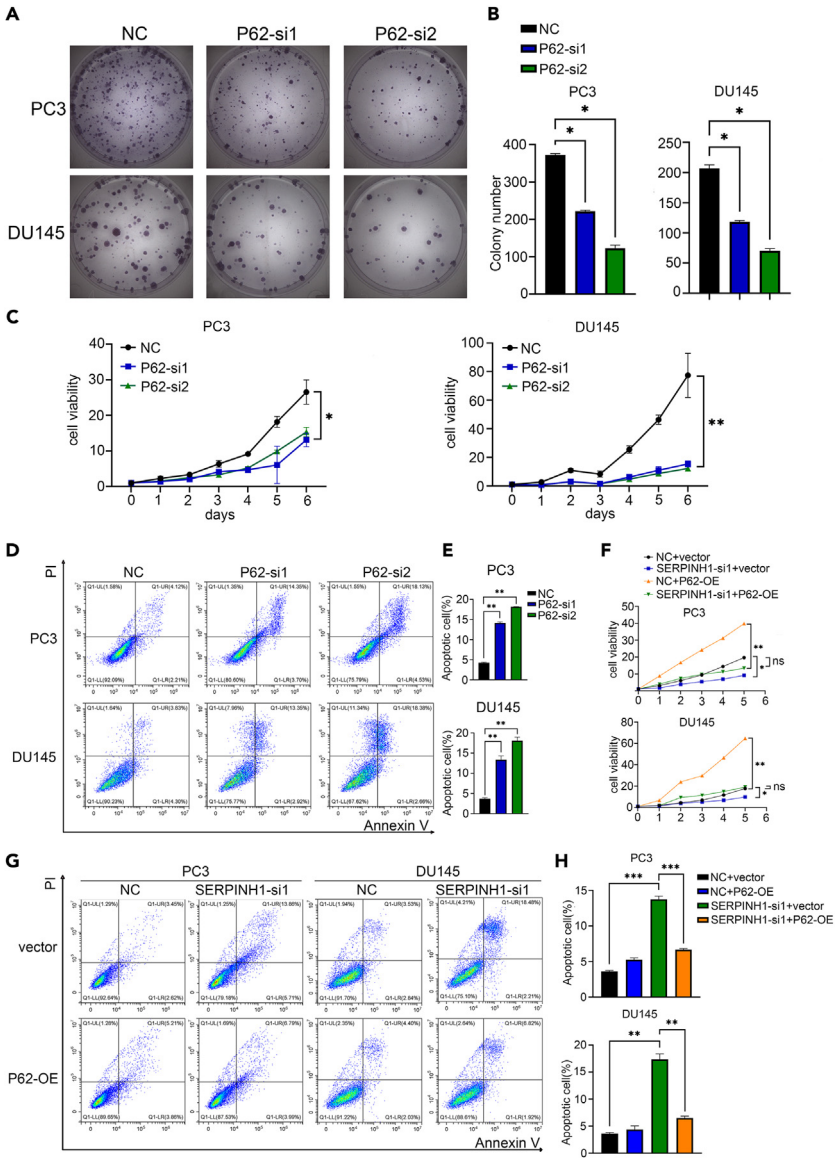

Figure 7. Effects of SERPINH1 knockdown on proliferation and apoptosis are recovered by P62 overexpression

(A) Colony-formation results of P62 knockdown cells.

(B) Histograms of the colony-formation results of P62 knockdown cells.

(C) Cell viability of P62 knockdown cells.

(D) Annexin V/PI apoptotic assays of P62 knockdown cells.

(E) Histograms of the percentage of Annexin V/PI staining cells.

(F) Cell viability SERPINH1 knockdown-P62 overexpressing cells.

(G) Annexin V/PI apoptotic results of these two kinds of transfected cells.

(H) Histograms of the percentage of double-stained cells. Data are represented as mean ± SD. (ns, no significant, *$p < 0.05$, **$p < 0.01$, ***$p < 0.001$).

enhanced P62 accumulation.[43] Similarly, our results demonstrated that SERPINH1 inhibits proteasomal degradation of P62, hence we hypothesized that the interaction between SERPINH1 and P62 may include modulation of ubiquitination degradation. There is a close relationship between ubiquitination and intracellular protein degradation. Three enzymes play a regulatory role in this process. Typically, ubiquitin ligase E3 identifies target proteins and is necessary for ubiquitination. The particular E3 ubiquitin ligases responsible for the SERPINH1-knockdown-mediated degradation of the P62 protein are unclear. However, we observed that the crossover of MS of SERPINH1 in two PCa cell lines indicated an E3 ligase, TRIM21. Both SERPINH1 and P62 interacted with TRIM21, and TRIM21 promoted the ubiquitination of both SERPINH1 and P62. In line with this, TRIM21 is considered to be a P62-specific E3 ligase ubiquitination enzyme that regulates self-oligomerization and localization of P62.[24,44] Our study demonstrated that an elevation in SERPINH1 significantly impaired the interaction between P62 and TRIM21, but

a knockdown of SERPINH1 significantly increased the interaction. From this, we infer that SERPINH1 may bind to P62 and form a protein dimer and that the binding site of P62 between TRIM21 is overlapped by the mutual binding, which prevents P62 ubiquitination by TRIM21 and reduces the ubiquitination proteasome degradation of P62. Further immunohistochemical staining of bone metastases in nude mice validated this protein expression correlation. Thus, in this study, we described a unique post-translational modification of P62 by SERPINH1; however, the regulatory mechanism needs further investigation.

Conclusions

This study demonstrated the underlying mechanism SERPINH1 inhibited the ubiquitination degradation of P62 in a K63-linkage ubiquitination manner. SERPINH1 promote PCa bone metastasis based on acceleration of PCa cell proliferation and inhibition of P62-dependent apoptosis; hence, it could represent a curative candidate for PCa patients with bone metastases.

Limitations of the study

The regulatory mechanism needs further investigation. Further experiment is needed to determine the inhibition of P62-dependent apoptosis by SERPINH1 plays a role in which stage of PCa bone metastasis.

STAR★METHODS

Detailed methods are provided in the online version of this paper and include the following:

- KEY RESOURCES TABLE
- RESOURCES AVAILABILITY
  - Lead contact
  - Materials availability
  - Data and code availability
- EXPERIMENTAL MODEL AND STUDY PARTICIPANT DETAILS
  - Animals
  - Specimens
  - Cell lines
- METHOD DETAILS
  - Cells transfection
  - Construction of stable cell lines
  - Intersection analysis of differentially expressed genes
  - Cells proliferation assays and colony formation assay
  - Cells migration assay
  - Immunofluorescence staining and imaging
  - Cells apoptosis assay
  - RNA extraction and real-time quantitative polymerase chain reaction
  - Co-immunoprecipitation (Co-IP) and western blot assay
  - Bone metastasis xenograft
  - Immunohistochemistry
  - TUNEL assay
  - GST pulldown assay
  - Sensitized emission FRET microscopy
  - Exogenous COL1 treatment assay
- QUANTIFICATION AND STATISTICAL ANALYSIS

SUPPLEMENTAL INFORMATION

Supplemental information can be found online at https://doi.org/10.1016/j.isci.2024.110427.

ACKNOWLEDGMENTS

This work was supported by grants from Guangdong Science and Technology Department (2017B030314026), Guangdong Province Key Laboratory of Malignant Tumor Epigenetics and Gene Regulation (no.: 2020B1212060018OF006), and Guangdong Provincial Clinical Research Center for Urological Diseases (2020B1111170006). Special thanks to Tian Qiao and Xiaojuan Wang from the Bioinformatics and Omics Center, SYSMH, who performed mass spectrometry analysis.

This work was supported by grants from the National Natural Science Foundation of China (82372912, 81802527), National Key Research and Development Program of China (2022YFC3602900), and Beijing Bethune Charitable Foundation (mnzl202026) to Y.L. and from the National Natural Science Foundation of China (no.: 81772733, 81972384). This work was supported by the National key R&D plan of China

(2022YFC3602904), the National Natural Science Foundation of China (no.: 81974395, 82173036), Key R&D Plan of Guangdong Province (no.: 2023B1111030006), International Science and technology cooperation project plan of Guangdong Province (no.: 2021A0505030085), Sun Yat-Sen University Clinical Research 5010 Program (no.: 2019005), Beijing Bethune Charitable Foundation (mnzl202001), Guangzhou Science and Technology Key R&D Project (202206010117), Beijing Xisike Clinical Oncology Research Foundation (Y-MSDZD2022-0760, Y-tongshu2021/ms-0162), and the open research funds from the Sixth Affiliated Hospital of Guangzhou Medical University and Qingyuan People's Hospital to H.H. This work was supported by Guangdong scientific research projects (2021A1515010223) to Z.G., Guangdong Provincial Clinical Research Center for Urological Diseases (2020B1111170006), and Guangdong Science and Technology Department (2020B1212060018).

AUTHOR CONTRIBUTIONS

Conceptualization, Y.L., C.T., Z.G., and H.H.; data curation, C.T., Y.L., K.L., S.P., Z.G., and H.H.; formal analysis, C.T., M.-y.S., and S.P.; funding acquisition, Y.L., K.L., Z.G., and H.H.; investigation, Y.L., B.C., Y.W., L.Z., and S.P.; methodology, C.T., Y.L., S.L., Y.C., B.C., and Y.R.; project administration, Y.L., K.L., Z.G., and H.H.; resources, Y.L., Z.L., L.Z., S.P., and H.H.; software, L.L., Y.C., B.C., J.Z., S.L., H.Z., and Z.L.; supervision, Y.L., K.L., S.P., Z.G., and H.H.; validation, Y.L., J.Z., and Z.G.; visualization, L.L., Y.C., and S.L.; writing – original draft, C.T., L.L., and S.P.; writing – review and editing, C.T., Y.L., L.L., and S.P.

DECLARATION OF INTERESTS

The authors declare no competing interests.

Received: December 27, 2023
Revised: April 30, 2024
Accepted: June 28, 2024
Published: July 10, 2024

REFERENCES

1. Fizazi, K., Yang, J., Peleg, S., Sikes, C.R., Kreimann, E.L., Daliani, D., Olive, M., Raymond, K.A., Janus, T.J., Logothetis, C.J., et al. (2003). Prostate cancer cells-osteoblast interaction shifts expression of growth/survival-related genes in prostate cancer and reduces expression of osteoprotegerin in osteoblasts. Clin. Cancer Res. *9*, 2587–2597.
2. Guise, T.A., Mohammad, K.S., Clines, G., Stebbins, E.G., Wong, D.H., Higgins, L.S., Vessella, R., Corey, E., Padalecki, S., Suva, L., and Chirgwin, J.M. (2006). Basic mechanisms responsible for osteolytic and osteoblastic bone metastases. Clin. Cancer Res. *12*, 6213s–6216s. https://doi.org/10.1158/1078-0432.Ccr-06-1007.
3. Ottewell, P.D. (2016). The role of osteoblasts in bone metastasis. J. Bone Oncol. *5*, 124–127. https://doi.org/10.1016/j.jbo.2016.03.007.
4. David Roodman, G., and Silbermann, R. (2015). Mechanisms of osteolytic and osteoblastic skeletal lesions. BoneKEy Rep. *4*, 753. https://doi.org/10.1038/bonekey.2015.122.
5. Hanahan, D., and Weinberg, R.A. (2011). Hallmarks of cancer: the next generation. Cell *144*, 646–674. https://doi.org/10.1016/j.cell.2011.02.013.
6. Nagata, K. (2003). HSP47 as a collagen-specific molecular chaperone: function and expression in normal mouse development. Semin. Cell Dev. Biol. *14*, 275–282. https://doi.org/10.1016/j.semcdb.2003.09.020.
7. Ito, S., and Nagata, K. (2017). Biology of Hsp47 (Serpin H1), a collagen-specific molecular chaperone. Semin. Cell Dev. Biol. *62*, 142–151. https://doi.org/10.1016/j.semcdb.2016.11.005.
8. Yang, Q., Liu, S., Tian, Y., Hasan, C., Kersey, D., Salwen, H.R., Chlenski, A., Perlman, E.J., and Cohn, S.L. (2004). Methylation-associated silencing of the heat shock protein 47 gene in human neuroblastoma. Cancer Res. *64*, 4531–4538. https://doi.org/10.1158/0008-5472.Can-04-0956.
9. Xiong, G., Chen, J., Zhang, G., Wang, S., Kawasaki, K., Zhu, J., Zhang, Y., Nagata, K., Li, Z., Zhou, B.P., and Xu, R. (2020). Hsp47 promotes cancer metastasis by enhancing collagen-dependent cancer cell-platelet interaction. Proc. Natl. Acad. Sci. USA *117*, 3748–3758. https://doi.org/10.1073/pnas.1911951117.
10. Manley, S., Williams, J.A., and Ding, W.X. (2013). Role of p62/SQSTM1 in liver physiology and pathogenesis. Exp. Biol. Med. *238*, 525–538. https://doi.org/10.1177/1535370213489446.
11. Moscat, J., and Diaz-Meco, M.T. (2012). p62: a versatile multitasker takes on cancer. Trends Biochem. Sci. *37*, 230–236. https://doi.org/10.1016/j.tibs.2012.02.008.
12. Moscat, J., Diaz-Meco, M.T., and Wooten, M.W. (2007). Signal integration and diversification through the p62 scaffold protein. Trends Biochem. Sci. *32*, 95–100. https://doi.org/10.1016/j.tibs.2006.12.002.
13. Cai-McRae, X., Zhong, H., and Karantza, V. (2015). Sequestosome 1/p62 facilitates HER2-induced mammary tumorigenesis through multiple signaling pathways. Oncogene *34*, 2968–2977. https://doi.org/10.1038/onc.2014.244.
14. Valencia, T., Kim, J.Y., Abu-Baker, S., Moscat-Pardos, J., Ahn, C.S., Reina-Campos, M., Duran, A., Castilla, E.A., Metallo, C.M., Diaz-Meco, M.T., and Moscat, J. (2014). Metabolic reprogramming of stromal fibroblasts through p62-mTORC1 signaling promotes inflammation and tumorigenesis. Cancer Cell *26*, 121–135. https://doi.org/10.1016/j.ccr.2014.05.004.
15. Inami, Y., Waguri, S., Sakamoto, A., Kouno, T., Nakada, K., Hino, O., Watanabe, S., Ando, J., Iwadate, M., Yamamoto, M., et al. (2011). Persistent activation of Nrf2 through p62 in hepatocellular carcinoma cells. J. Cell Biol. *193*, 275–284. https://doi.org/10.1083/jcb.201102031.
16. Inoue, D., Suzuki, T., Mitsuishi, Y., Miki, Y., Suzuki, S., Sugawara, S., Watanabe, M., Sakurada, A., Endo, C., Uruno, A., et al. (2012). Accumulation of p62/SQSTM1 is associated with poor prognosis in patients with lung adenocarcinoma. Cancer Sci. *103*, 760–766. https://doi.org/10.1111/j.1349-7006.2012.02216.x.
17. Yan, X.Y., Zhang, Y., Zhang, J.J., Zhang, L.C., Liu, Y.N., Wu, Y., Xue, Y.N., Lu, S.Y., Su, J., and Sun, L.K. (2017). p62/SQSTM1 as an oncotarget mediates cisplatin resistance through activating RIP1-NF-κB pathway in human ovarian cancer cells. Cancer Sci. *108*, 1405–1413. https://doi.org/10.1111/cas.13276.
18. Takamura, A., Komatsu, M., Hara, T., Sakamoto, A., Kishi, C., Waguri, S., Eishi, Y., Hino, O., Tanaka, K., and Mizushima, N. (2011). Autophagy-deficient mice develop multiple liver tumors. Genes Dev. *25*, 795–800. https://doi.org/10.1101/gad.2016211.
19. Taniguchi, K., Yamachika, S., He, F., and Karin, M. (2016). p62/SQSTM1-Dr. Jekyll and Mr. Hyde that prevents oxidative stress but promotes liver cancer. FEBS Lett. *590*, 2375–2397. https://doi.org/10.1002/1873-3468.12301.
20. Liang, X., Yao, J., Cui, D., Zheng, W., Liu, Y., Lou, G., Ye, B., Shui, L., Sun, Y., Zhao, Y., and Zheng, M. (2023). The TRAF2-p62 axis promotes proliferation and survival of liver cancer by activating mTORC1 pathway. Cell Death Differ. *30*, 1550–1562. https://doi.org/10.1038/s41418-023-01164-7.
21. Wu, Q., Zhang, H., You, S., Xu, Z., Liu, X., Chen, X., Zhang, W., Ye, J., Li, P., and Zhou, X. (2023). NEDD4L inhibits migration, invasion,

cisplatin resistance and promotes apoptosis of bladder cancer cells by inactivating the p62/Keap1/Nrf2 pathway. Environ. Toxicol. *38*, 1678–1689. https://doi.org/10.1002/tox.23796.

22. Noguchi, T., Sekiguchi, Y., Shimada, T., Suzuki, W., Yokosawa, T., Itoh, T., Yamada, M., Suzuki, M., Kurokawa, R., Hirata, Y., and Matsuzawa, A. (2023). LLPS of SQSTM1/p62 and NBR1 as outcomes of lysosomal stress response limits cancer cell metastasis. Proc. Natl. Acad. Sci. USA *120*, e2311282120. https://doi.org/10.1073/pnas.2311282120.
23. Wang, F., Zhang, Y., Shen, J., Yang, B., Dai, W., Yan, J., Maimouni, S., Daguplo, H.Q., Coppola, S., Gao, Y., et al. (2021). The Ubiquitin E3 Ligase TRIM21 Promotes Hepatocarcinogenesis by Suppressing the p62-Keap1-Nrf2 Antioxidant Pathway. Cell. Mol. Gastroenterol. Hepatol. *11*, 1369–1385. https://doi.org/10.1016/j.jcmgh.2021.01.007.
24. Jin, J., Meng, X., Huo, Y., and Deng, H. (2021). Induced TRIM21 ISGylation by IFN-β enhances p62 ubiquitination to prevent its autophagosome targeting. Cell Death Dis. *12*, 697. https://doi.org/10.1038/s41419-021-03989-x.
25. Kuchimaru, T., Kataoka, N., Nakagawa, K., Isozaki, T., Miyabara, H., Minegishi, M., Kadonosono, T., and Kizaka-Kondoh, S. (2018). A reliable murine model of bone metastasis by injecting cancer cells through caudal arteries. Nat. Commun. *9*, 2981. https://doi.org/10.1038/s41467-018-05366-3.
26. Wang, L., Li, C., Zhan, H., Li, S., Zeng, K., Xu, C., Zou, Y., Xie, Y., Zhan, Z., Yin, S., et al. (2024). Targeting the HSP47-collagen axis inhibits brain metastasis by reversing M2 microglial polarization and restoring anti-tumor immunity. Cell Rep. Med. *5*, 101533. https://doi.org/10.1016/j.xcrm.2024.101533.
27. Bussard, K.M., Gay, C.V., and Mastro, A.M. (2008). The bone microenvironment in metastasis; what is special about bone? Cancer Metastasis Rev. *27*, 41–55. https://doi.org/10.1007/s10555-007-9109-4.
28. Cortés-Hernández, L.E., Eslami, S.Z., and Alix-Panabières, C. (2020). Circulating tumor cell as the functional aspect of liquid biopsy to understand the metastatic cascade in solid cancer. Mol. Aspects Med. *72*, 100816. https://doi.org/10.1016/j.mam.2019.07.008.
29. Boerrigter, E., Groen, L.N., Van Erp, N.P., Verhaegh, G.W., and Schalken, J.A. (2020). Clinical utility of emerging biomarkers in prostate cancer liquid biopsies. Expert Rev. Mol. Diagn. *20*, 219–230. https://doi.org/10.1080/14737159.2019.1675515.
30. Mastro, A.M., Gay, C.V., Welch, D.R., Donahue, H.J., Jewell, J., Mercer, R., DiGirolamo, D., Chislock, E.M., and Guttridge, K. (2004). Breast cancer cells induce osteoblast apoptosis: a possible contributor to bone degradation. J. Cell. Biochem. *91*, 265–276. https://doi.org/10.1002/jcb.10746.
31. Yin, J.J., Pollock, C.B., and Kelly, K. (2005). Mechanisms of cancer metastasis to the bone. Cell Res. *15*, 57–62. https://doi.org/10.1038/sj.cr.7290266.
32. Su, Z., Yang, Z., Xu, Y., Chen, Y., and Yu, Q. (2015). Apoptosis, autophagy, necroptosis, and cancer metastasis. Mol. Cancer *14*, 48. https://doi.org/10.1186/s12943-015-0321-5.
33. Roca, H., Jones, J.D., Purica, M.C., Weidner, S., Koh, A.J., Kuo, R., Wilkinson, J.E., Wang, Y., Daignault-Newton, S., Pienta, K.J., et al. (2018). Apoptosis-induced CXCL5 accelerates inflammation and growth of prostate tumor metastases in bone. J. Clin. Invest. *128*, 248–266. https://doi.org/10.1172/jci92466.
34. Li, X., Chen, T., Shi, Q., Li, J., Cai, S., Zhou, P., Zhong, Y., and Yao, L. (2015). Angiopoietin-like 4 enhances metastasis and inhibits apoptosis via inducing bone morphogenetic protein 7 in colorectal cancer cells. Biochem. Biophys. Res. Commun. *467*, 128–134. https://doi.org/10.1016/j.bbrc.2015.09.104.
35. Li, R., Shi, Y., Zhao, S., Shi, T., and Zhang, G. (2019). NF-κB signaling and integrin-β1 inhibition attenuates osteosarcoma metastasis via increased cell apoptosis. Int. J. Biol. Macromol. *123*, 1035–1043. https://doi.org/10.1016/j.ijbiomac.2018.11.003.
36. Bao, X., Ren, T., Huang, Y., Ren, C., Yang, K., Zhang, H., and Guo, W. (2017). Bortezomib induces apoptosis and suppresses cell growth and metastasis by inactivation of Stat3 signaling in chondrosarcoma. Int. J. Oncol. *50*, 477–486. https://doi.org/10.3892/ijo.2016.3806.
37. Zhu, J., Xiong, G., Fu, H., Evers, B.M., Zhou, B.P., and Xu, R. (2015). Chaperone Hsp47 Drives Malignant Growth and Invasion by Modulating an ECM Gene Network. Cancer Res. *75*, 1580–1591. https://doi.org/10.1158/0008-5472.Can-14-1027.
38. Kawasaki, K., Ushioda, R., Ito, S., Ikeda, K., Masago, Y., and Nagata, K. (2015). Deletion of the collagen-specific molecular chaperone Hsp47 causes endoplasmic reticulum stress-mediated apoptosis of hepatic stellate cells. J. Biol. Chem. *290*, 3639–3646. https://doi.org/10.1074/jbc.M114.592139.
39. Chang, M.A., Morgado, M., Warren, C.R., Hinton, C.V., Farach-Carson, M.C., and Delk, N.A. (2014). p62/SQSTM1 is required for cell survival of apoptosis-resistant bone metastatic prostate cancer cell lines. Prostate *74*, 149–163. https://doi.org/10.1002/pros.22737.
40. Zhao, Y., Zhu, Q., Bu, X., Zhou, Y., Bai, D., Guo, Q., Gao, Y., and Lu, N. (2020). Triggering apoptosis by oroxylin A through caspase-8 activation and p62/SQSTM1 proteolysis. Redox Biol. *29*, 101392. https://doi.org/10.1016/j.redox.2019.101392.
41. Morselli, E., Galluzzi, L., Kepp, O., Vicencio, J.M., Criollo, A., Maiuri, M.C., and Kroemer, G. (2009). Anti- and pro-tumor functions of autophagy. Biochim. Biophys. Acta *1793*, 1524–1532. https://doi.org/10.1016/j.bbamcr.2009.01.006.
42. Siswanto, F.M., Mitsuoka, Y., Nakamura, M., Oguro, A., and Imaoka, S. (2022). Nrf2 and Parkin-Hsc70 regulate the expression and protein stability of p62/SQSTM1 under hypoxia. Sci. Rep. *12*, 21265. https://doi.org/10.1038/s41598-022-25784-0.
43. Gong, L., Wang, K., Wang, M., Hu, R., Li, H., Gao, D., and Lin, M. (2021). CUL5-ASB6 Complex Promotes p62/SQSTM1 Ubiquitination and Degradation to Regulate Cell Proliferation and Autophagy. Front. Cell Dev. Biol. *9*, 684885. https://doi.org/10.3389/fcell.2021.684885.
44. Pan, J.A., Sun, Y., Jiang, Y.P., Bott, A.J., Jaber, N., Dou, Z., Yang, B., Chen, J.S., Catanzaro, J.M., Du, C., et al. (2016). TRIM21 Ubiquitylates SQSTM1/p62 and Suppresses Protein Sequestration to Regulate Redox Homeostasis. Mol. Cell *61*, 720–733. https://doi.org/10.1016/j.molcel.2016.02.007.
45. Peng, S., Chen, X., Huang, C., Yang, C., Situ, M., Zhou, Q., Ling, Y., Huang, H., Huang, M., Zhang, Y., et al. (2022). UBE2S as a novel ubiquitinated regulator of p16 and β-catenin to promote bone metastasis of prostate cancer. Int. J. Biol. Sci. *18*, 3528–3543. https://doi.org/10.7150/ijbs.72629.
46. Iglesias-Gato, D., Thysell, E., Tyanova, S., Crnalic, S., Santos, A., Lima, T.S., Geiger, T., Cox, J., Widmark, A., Bergh, A., et al. (2018). The Proteome of Prostate Cancer Bone Metastasis Reveals Heterogeneity with Prognostic Implications. Clin. Cancer Res. *24*, 5433–5444. https://doi.org/10.1158/1078-0432.Ccr-18-1229.
47. Zhou, Q., Chen, X., He, H., Peng, S., Zhang, Y., Zhang, J., Cheng, L., Liu, S., Huang, M., Xie, R., et al. (2021). WD repeat domain 5 promotes chemoresistance and Programmed Death-Ligand 1 expression in prostate cancer. Theranostics *11*, 4809–4824. https://doi.org/10.7150/thno.55814.

STAR★METHODS

KEY RESOURCES TABLE

REAGENT or RESOURCE	SOURCE	IDENTIFIER
Antibodies		
SERPINH1 Antibody	Proteintech	Cat#67863-1-IG
P62 Antibody	Proteintech	Cat#66184-1-IG
TRIM21 Antibody	Proteintech	Cat#12108-1-AP
DYKDDDDK Antibody	Proteintech	Cat#66008-3-IG
HA Antibody	Proteintech	Cat#66006-2-Ig
Ubiquitin Antibody	Proteintech	Cat#10201-2-AP
GAPDH Antibody	Proteintech	Cat#10494-1-AP
HRP-labeled Goat Anti-Mouse IgG(H + L)	CWBIO	Cat#CW0102S
DyLight 488, Goat Anti Mouse IgG	Immunoway	Cat#RS23210
Dylight 649, Goat Anti Mouse IgG	Immunoway	Cat#RS23610
HRP-labeled Goat Anti-Rabbit IgG(H + L)	CWBIO	Cat#CW0103S
Chemicals, peptides, and recombinant proteins		
DMEM	Gibco	Cat#11965092
DAPI	Beyotime	Cat#P0131-25
Enhanced chemiluminescence	Proteintech	Cat#PK10003
FBS	Sigma Aldrich	Cat#F8318-500ML
Streptomycin penicillin	Sigma Aldrich	Cat#V900929-100ML
PrimerScript RT-PCR kit	Vazyme	R222-01
PIERCE IP LYSIS BUFFER	Invitrogen	Cat#87787
Pierce™ GST Protein Interaction Pull-Down Kit	Thermo Scientific, Waltham, MA	Cat#21516
QuickBlockTM immunostaining sealer	Beyotime	Cat#P0260
Recombinant Human Collagen I alpha 1/COL1A1 Protein	Abclonal china	Cat#RP01842
TUNEL FITC Apoptosis Detection Kit	Vazyme	Cat#A111-01
Triton X-100	Beyotime	Cat#P0096-500 mL
PIERCE IP LYSIS BUFFER	Invitrogen	Cat#87787
Deposited data		
Diego proteome datasets	Clinical Cancer Research portal	https://aacrjournals.org/clincancerres/article/24/21/5433/281650/The-Proteome-of-Prostate-Cancer-Bone-Metastasis?searchresult=1
RNA-seq	The National Genome Data Center databse	HRA002360
RNA-seq	Gene Expression Omnibus database	GSE77930
Experimental models: cell lines		
Human: PC3	ATCC	Cat#CRL-1435
Human: DU145	ATCC	Cat#HTB81
Human: 293T	CRCPUMC, Beijing, China	N/A
Experimental models: organisms/strains		
BALB/c nude	Shanghai SLAC Co. Ltd	N/A

(*Continued on next page*)

Continued

REAGENT or RESOURCE	SOURCE	IDENTIFIER
Oligonucleotides		
Primer for SERPINH1, P62, TRIM21, GAPDH, see Table S5	N/A	N/A
siRNA for SERPINH1, P62, TRIM21, see Table S4	N/A	N/A
shRNA for SERPINH1 see Table S4	N/A	N/A
Recombinant DNA		
Plasmid: pCDH-CMV-MCS-EF1a-puro	Guangzhou IGE Biotechnology	N/A
Plasmid: pCDH-CMV-3xFlag-Homo-SERPINH1-EF1a-puro	Guangzhou IGE Biotechnology	N/A
Plasmid: pGEX-4T-1	Guangzhou IGE Biotechnology	N/A
Plasmid: pGEX-4T-1-Homo-SERPINH1	Guangzhou IGE Biotechnology	N/A
Plasmid: pcDNA3.1(+)	Guangzhou IGE Biotechnology	N/A
Plasmid: pcDNA3.1(+)-Homo-SQSTM1	Guangzhou IGE Biotechnology	N/A
Plasmid: pcDNA3.1(+)-Homo-SERPINH1-TagCFP	Guangzhou IGE Biotechnology	N/A
Plasmid: pcDNA3.1(+)-Homo-SQSTM1-TagYFP	Guangzhou IGE Biotechnology	N/A
Plasmid: pLKO.1-scramble-puro	Guangzhou IGE Biotechnology	N/A
Plasmid: pLKO.1-Homo-SERPINH1-sh1-puro	Guangzhou IGE Biotechnology	N/A
Plasmid: pLKO.1-Homo-SERPINH1-sh2-puro	Guangzhou IGE Biotechnology	N/A
Software and algorithms		
Beckman Coulter CytoFlex S	Beckman	N/A
BRUKER software 7.1.3	Bruker	N/A
GraphPad Prism 9.3	GraphPad software	N/A
Leica TCS SP8 microscope	Leica	N/A
Micro-computed tomography (μCT)	Bruker	N/A
SmartChemi 910	SinSage Technology Co., Ltd.	N/A
SPSS 24.0	IBM SPSS software	N/A
X-ray	Bruker MI	N/A

RESOURCES AVAILABILITY

Lead contact

Further information and requests for resources and reagents should be directed to and will be fulfilled by the lead contact, Dr. Hai Huang (huangh9@mail.sysu.edu.cn).

Materials availability

This paper did not generate new reagents or materials.

Data and code availability

- RNA and protein extraction procedures and clinicopathological features of patients are detailed in our previous study.[45] Two experienced pathologists performed immunohistochemistry staining on all samples to make the diagnosis. The National Genome Data Center received all RNA-seq data (HRA002360). The GEO gateway provided GSE77930 with entire human genome expression oligonucleotide microarray data (https://www.ncbi.nlm.nih.gov/geo/). Diego proteome datasets were retrieved from the Clinical Cancer Research portal (https://aacrjournals.org/clincancerres).
- This study did not report any original code.
- Any additional information required to reanalyze the data reported in this paper was available from the lead contact upon request.

EXPERIMENTAL MODEL AND STUDY PARTICIPANT DETAILS

Animals

Sun Yat-sen University Institution Animal Care and Use Committee (SYSU-IACUC-2021-000041) approved all mouse research. Shanghai SLAC Co. Ltd provided the 4w male BALB/c nude mouse.

Specimens

The study was conducted in accordance with the Declaration of Helsinki. This study comprised 103 PCa tissue specimens that were formalin-fixed and paraffin-embedded from SYSUCC between January 2005 and 2018. Two senior pathologists confirmed the diagnosis of these samples using immunohistochemical staining. Informed consent was obtained from all subjects involved in the study. Sun Yat-sen University Ethics Committee (SYSEC-KY-KS-2020-201) authorized the study. Clinical and demographic details of all participants were provided in Table S6.

Cell lines

The experimental investigation utilized PC3 and DU145 cells from the American Typical Culture Collection Center (ATCC, VA, USA) and 293T cells from Beijing Union Medical College (CRCPUMC, Beijing, China), all maintained in liquid nitrogen. PC3 cells were cultivated in RPMI 1640 and the other two in DMEM (Gibco, Shanghai, China). Both media contain 1% streptomycin penicillin and 10% FBS (Sigma Aldrich, USA). Cells were cultured under standard conditions. At the time of experimental detection, all cell lines did not contain mycoplasma. Short tandem repetitions (STR) were performed on PC3 and DU145 to confirm the lack of misidentification or contamination.

METHOD DETAILS

Cells transfection

Zuoke (Guangzhou, China) provided the plasmid for the amplification of SERPINH1 or P62. GenePharma (Shanghai, China) provided the siRNAs for targeting negative control, SERPINH1, P62, or TRIM21. As per the manufacturer's recommendations, siRNAs and plasmids were transfected into PC3 or DU145 cells by Lipofectamine RNAiMAX and Lipofectamine 3000, respectively.

Construction of stable cell lines

SERPINH1 or P62's CDS and shRNA sequences were introduced into pCDH-puro and pLKO-puro plasmid respectively and co-transfected into 293T cells with pMD2G and pspAX2 in 10 cm plates to produce lentivirus. After transfection for 72 h, a 0.45μm polyether sulfone membrane was used to collect and filter the supernatant of transfected 293T cells. PC3-luciferase cells were infected with untargeted control, SERPINH1#sh1 and SERPINH1#sh2, or pCDH-vector or SERPINH1-OE, respectively. Virus infection was repeated thrice every 12 h, and stable knockdown or overexpressing cells were screened using puromycin. qRT-PCR and western blotting demonstrated SERPINH1 knockdown or overexpression at least five days post-infection.

Intersection analysis of differentially expressed genes

SYSU-RNA sequencing and SYSU proteomic datasets were previously established by our research group. SYSU-RNA sequencing[45] was obtained via whole-transcriptome sequencing of six bone metastases of PCa specimens, six bone metastatic PCa *in situ* specimens, and seven primary PCa *in situ* specimens from our hospital. The SYSU proteomics datasets previously established by our research group were obtained via quantitative proteomic analysis of bone metastases in 11 cases of PCa in our hospital. The GEO gateway provided GSE77930 with entire human genome expression oligonucleotide microarray data (https://www.ncbi.nlm.nih.gov/geo/). Diego proteome datasets were retrieved from the Clinical Cancer Research portal (https://aacrjournals.org/clincancerres).[46] Differentially expressed genes (DEGs) had a Log2(Fold Change) > 1 and a $p < 0.05$.

Cells proliferation assays and colony formation assay

The CCK8 and colony formation assays were performed to determine cell viability as previously described.[45] OD was measured at 450 nm after incubating the CCK-8 reagent at 37°C for 2 h.

Cells migration assay

Cells were seeded into a six-well plate and subjected to appropriate treatments. When the cells reached 75% confluence, they were digested and passaged to obtain cell pellets. (2) Resuspend the cells in serum-free culture medium, count the cells, and dilute to a concentration of 2×10^5 cells/mL. Prepare a 24-well cell culture plate and place the chamber inside. Add 600μL of complete culture medium to the lower chamber and 200μL of cell suspension to the upper chamber. Place the plate back into the incubator for cultivation. DU145 cells require 12–16 h of cultivation, while PC3 cells require 60–72 h. Remove the upper layer of culture medium from the chamber, transfer the chamber to a well containing 4% paraformaldehyde, and fix for 15–20 min. Move the chamber to a well with 0.5% crystal violet staining solution and stain for 10–15 min. Use a damp cotton swab to wipe off the upper layer of cells in the chamber, then rinse the chamber under running water to remove residual crystal violet staining solution. Allow it to dry at room temperature, and then use a microscope for imaging, documentation, and counting.

Immunofluorescence staining and imaging

Transfected cells were fixed for 30 min with 4% paraformaldehyde, permeabilized for 10 min with Triton X-100 (Beyotime, P0096-500 mL), then blocked with QuickBlockTM immunostaining sealer (Beyotime, P0260) and incubated with the anti-SERPINH1 antibody at 4°C overnight, then stained with Dylight488-conjugated secondary antibody for 1 h and washed thoroughly with PBS. Whereafter they were incubated with the anti-P62 antibody at 4°C overnight, stained with Dylight649-conjugated secondary antibody the next day, and finally stained with DAPI (Beyotime, P0131-25). A Zeiss LSM800 airscan laser confocal microscope was used for imaging.

Cells apoptosis assay

PC3 or DU145 cells (1×10^6) transfected with siRNA or plasmids, or both. 72 h after transfection, supernatants were collected. After being digested with EDTA-free trypsin, the remaining cells were combined with the supernatants, and subsequently stained via Annexin V and PI for 10 min. The cell apoptosis rate was detected based on Flow cytometry (Beckman Coulter CytoFlex S).

RNA extraction and real-time quantitative polymerase chain reaction

As previously mentioned, RNA extraction and RT-PCR were performed.[47] The PrimerScript RT-PCR kit (Vazyme) was applied to reverse-transcribe total RNA (1 μg), and relative mRNA expression was calculated by comparison basis of GAPDH. Table S5 lists the primers used in this study.

Co-immunoprecipitation (Co-IP) and western blot assay

PIERCE IP LYSIS BUFFER (Invitrogen, 87787) was used for protein extraction. Whole-cell lysates were divided into three parts: one-fifth for input and two-fifths incubated with the IgG or target antibody at 4°C for 12 h. The tube was spun with A/G beads (B23202) at 4°C for 2 h, and the beads were magnetically extracted and rinsed with lysis buffer five times. As previously mentioned, western blot experiments were performed.[47] Enhanced chemiluminescence (Proteintech, PK10003) and SmartChemi 910 were used to identify and image the target protein.

Bone metastasis xenograft

To generate PCa bone metastases, nude mice were injected with 2×10^6 puromycin screened SERPINH1 knockdown or SERPINH1 overexpression and respective control group PC3-Luc cells via the intra-caudal artery.[25] There were six mice in each group. Following that, to check bone metastases, all mice were observed and photographed once a week using the bioluminescent imaging (BLI) system and X-ray (Bruker MI). The X-ray image acquisition parameters were set to 10 s and 35 keV. The endpoint event was the total of BLI signals in either group $>1.5\times10^7$ determined by BRUKER software 7.1.3. The mice were under continuous surveillance until the endpoint event, at which point they were sacrificed by anesthesia overdose and cervical dislocation. Lower limb bone tissue containing malignancies was removed and stored in 10% neutral formalin. Micro-computed tomography (μCT) was performed on the dissected tissues using a Bruker skyscan1276. All dissected tissues were decalcified using an EDTA decalcification solution and embedded in paraffin.

Immunohistochemistry

Two independent pathologists assessed immunostaining intensity without knowledge of clinicopathological information or patient outcomes and counted the number of positively stained areas in the three representative fields at 400-folds. The product of the staining intensity score and positively stained region determines the immunoreactivity score (IRS) of the protein expression in each segment as previously described.[45] A high expression was identified as SERPINH1 IRS >100.

TUNEL assay

TUNEL FITC Apoptosis Detection Kit (A111-01, Vazyme) was utilized to identify apoptotic cells in the tissue samples obtained from mice. In brief, the tissue sections were subjected to dewaxing, hydration, permeabilization and incubation with the TUNEL reaction mixture for 1 h at 37°C temperatures. Subsequently, sections were washed twice with PBS for 5 min each and then subjected to incubation with DAPI for 5 min. Post incubation, the tissue sections were rinsed twice again. Observations were made using a ZEISS Scope fluorescence microscope (Oberkochen, Germany) and the TUNEL-positive cells were quantified using ImageJ software.

GST pulldown assay

The synthesis of glutathione S-transferase (GST) and a GST-SERPINH1 fusion protein was achieved by transfecting BL21 (DE3) competent cells with the pGEX-GST control vector and the pGEX-GST-SERPINH1 construct, respectively. Subsequently, protein production was stimulated by the addition of 0.5mM isopropyl β-D-1-thiogalactopyranoside (IPTG). The GST pull-down experiments were conducted in line with the guidelines provided in the Pierce GST Protein Interaction Pull-Down Kit (Thermo Scientific, Waltham, MA). In short, the recombinant GST-SERPINH1 or GST protein was mixed with Glutathione Agarose and kept at 4°C for 2 h. Following 7–8 washes using the recommended wash buffer (a mixture of TBS and Pull-Down Lysis Buffer in a 1:1 ratio), the Glutathione Agarose was then exposed to 293T cell lysate at 4°C for another 2 h, with an additional 7–8 washes using the same buffer. Analysis of the samples was subsequently carried out via Western blot technique.

Sensitized emission FRET microscopy

The Fluorescence Resonance Energy Transfer (FRET) assay was conducted with CFP serving as the FRET donor and YFP as the acceptor. We used confocal dishes to transfect SERPINH1-CFP plasmids and P62-YFP plasmids into 293T cells separately or together. After 24 h, we performing FRET sensitized emission (FRET-SE) experiments using the Leica TCS SP8 microscope. Briefly, we Define imaging conditions for the donor, FRET, and acceptor fluorescence, and acquire images to assess intensities and adjust settings. Next, we capture image sequences of the FRET sample, as well as separate controls for the donor only and acceptor only. Then, regions of interest (ROIs) were drawn in the control images to obtain calibration factors for correcting cross-talk between channels. The FRET efficiency (%) was calculated as: $E_A(i) = \frac{B-A\times\beta-C\times(\gamma-\alpha\times\beta)}{C\times(1-\beta\times\delta)}$.

Exogenous COL1 treatment assay

To address whether the collagen influenced the apoptosis induced by knockdown of SERPINH1, transfected PC3 or DU145 cells were treated with 4 mg/mL recombinant Human Collagen I alpha 1/COL1A1 Protein (RP01842, abclonal china) for 24h. Cells were harvested and sent for flow cytometry to determine cells apoptosis.

QUANTIFICATION AND STATISTICAL ANALYSIS

SPSS 24.0 and GraphPad Prism 9.3 was used to perform data statistics and analysis. The mean and standard deviation (xs) was used to express the quantitative data. Independent t-tests examined grouped differences. One-way ANOVA and Dunnett's comparison were used to compare quantitative data. Chi-squared test was used to compare numerical data. Kaplan-Meier calculated overall and progression-free survival. While the hazard ratios and 95% CI were calculated by the Cox hazards model with significant judgment criteria of $p < 0.05$.